Dynamic Imaging

Tomographic reconstruction, object recognition, classification, tracking...

Daniil Kazantsev

ITT9, 29.01.2019

Diamond Light Source

Two fast imaging examples and data modelling tool

1. Microstructural ice-cream melting/freezing processes

Data collected on I13 beamline of DLS by *E. Guo* et al. [1, 4]
https://www.diamond.ac.uk/Instruments/Imaging-and-Microscopy/I13.html

Two fast imaging examples and data modelling tool

1. Microstructural ice-cream melting/freezing processes

Data collected on I13 beamline of DLS by *E. Guo* et al. [1, 4]
https://www.diamond.ac.uk/Instruments/Imaging-and-Microscopy/I13.html

2. Microstructural dendritic grain growth in Mg alloys

Data collected on I13 beamline of DLS by *E. Guo* et al. [3, 2, 5]

Two fast imaging examples and data modelling tool

1. Microstructural ice-cream melting/freezing processes

Data collected on I13 beamline of DLS by *E. Guo* et al. [1, 4]
https://www.diamond.ac.uk/Instruments/Imaging-and-Microscopy/I13.html

2. Microstructural dendritic grain growth in Mg alloys

Data collected on I13 beamline of DLS by *E. Guo* et al. [3, 2, 5]

3. Modelling phantoms and tomographic data with artifacts

TomoPhantom software is able to model 2D-4D phantoms and their projection data with noise and some common imaging artifacts [6]
https://github.com/dkazanc/TomoPhantom

Looking into ice-cream structure

Looking into ice-cream structure

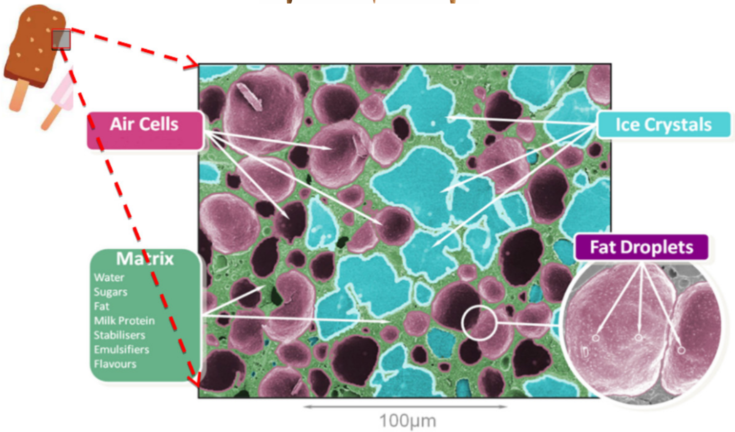

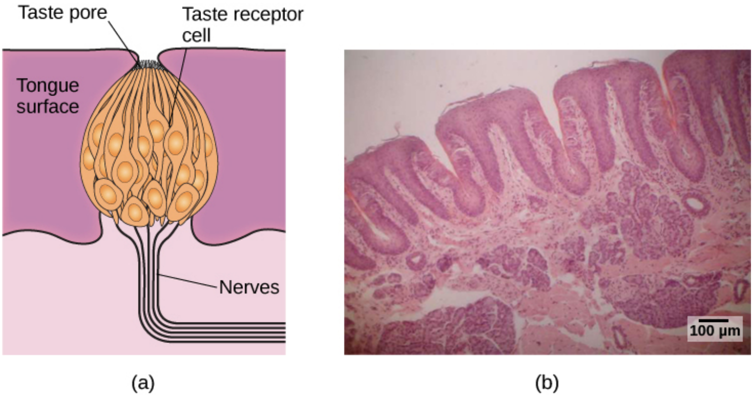

Figure 1: (a) a taste bud; (b) The micrograph shows a close-up view of tongue's surface

What causes the shape of ice-crystals to change?

Manufacturer

Transportation

Ice Cream Seller

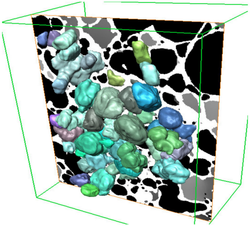

Smooth crystals

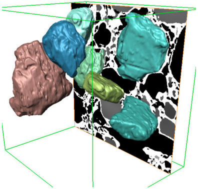

Rough crystals

The goal is to establish various morphological relationships in ice-cream microstructure as a function of time and temperature

Using thermal 'abuse' chamber

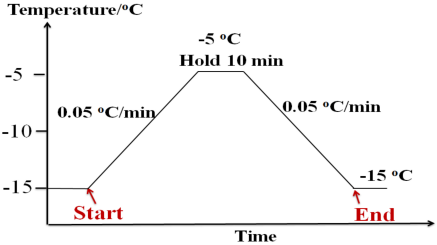

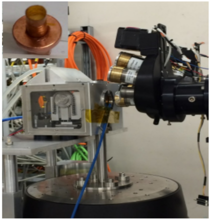

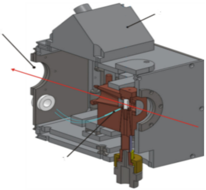

Direct (FBP) reconstruction

FBP reconstruction

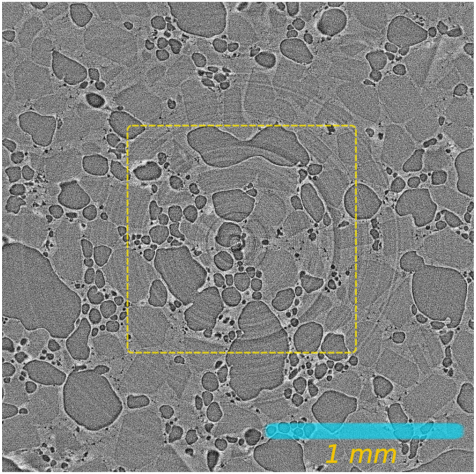

Cropped $1.5k^2$ pixels region, 900 proj.

zoomed region

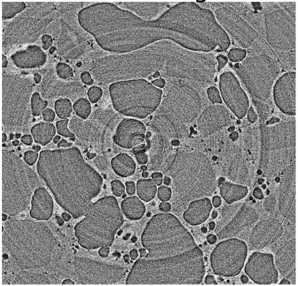

The list of issues:
- low contrast
- noise levels
- ring artifacts
- motion artifacts
- big data ($2k^3$ x 100)

Three-phases structure

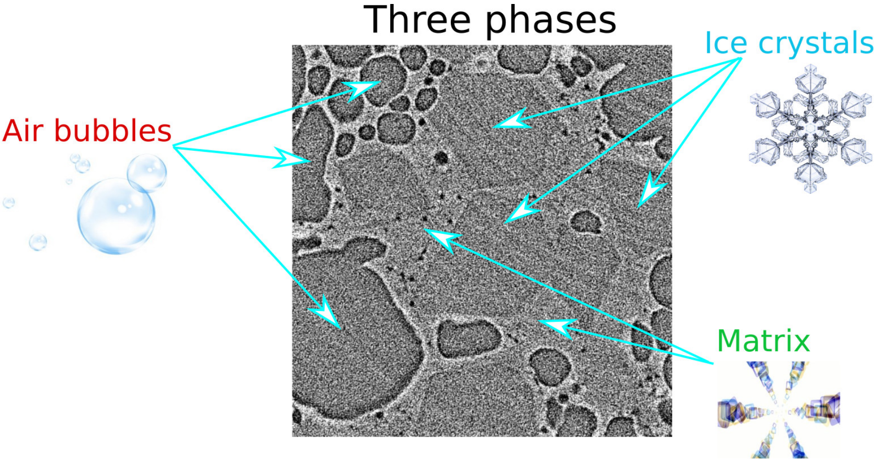

One solution to reach segmentable quality

We equalized intensity within separate phases by means of gradient-constrained 3D non-linear diffusion. Here we use the advantage of very sharp and clear boundaries of IR ice-matrix.

FIISTA-TV-L1(ring)

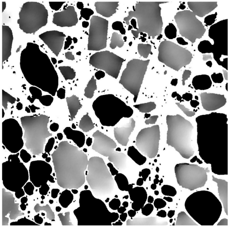

Input: cropped volume

size: 900 x 900 x 650 vox.

3D Constr. Diffusion

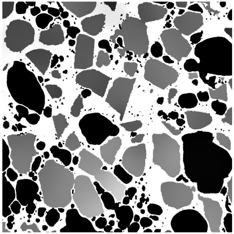

Output: processed volume with equalized intensities within each phase

GPU time: 1 hour
CPU time (24 cores) = 60h!

Segmentation

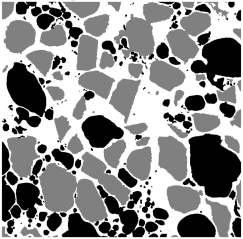

Result: segmented volume with three phases

3 values threhsolding +
some spots cleaning

Segmented 3-phases time-lapse

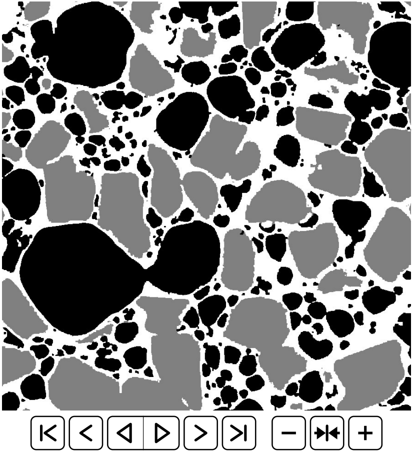

Dendritic growth experiments

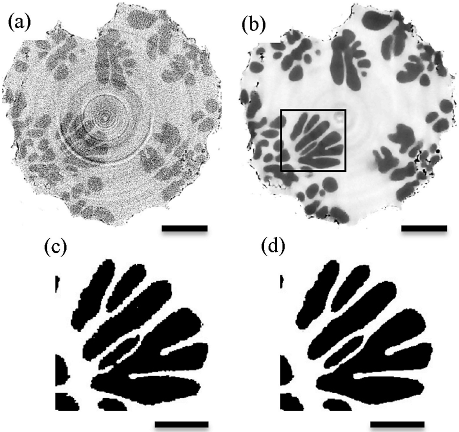

Reconstructed time-lapse dendritic data

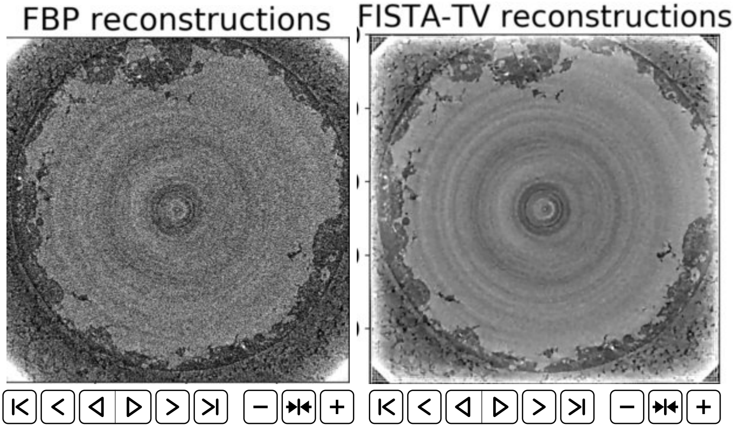

80 time-frames reconstructed with FBP (left) and iteratively (right).

TomoPhantom: software package to generate 2D–4D phantoms for CT image reconstruction algorithm benchmarks

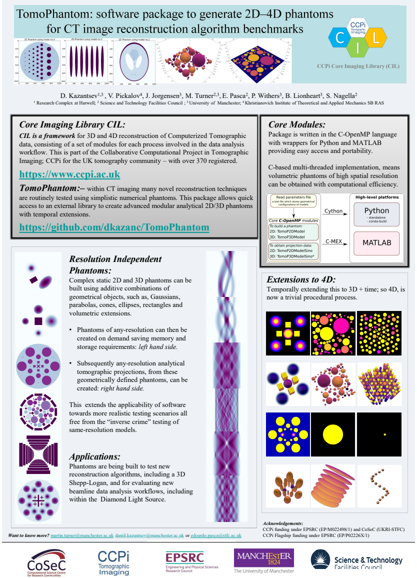

Fast tomographic imaging challenges

Very low signal-to-noise ratio, various errors in projections resulting in inaccurate reconstructions, motion artifacts.

1. Advanced image reconstruction techniques: mathematical methodology, practical challenges

Fast tomographic imaging challenges

Very low signal-to-noise ratio, various errors in projections resulting in inaccurate reconstructions, motion artifacts.

1. Advanced image reconstruction techniques: mathematical methodology, practical challenges
2. Better segmentation methods, object recognition, feature tracking, clustering and labeling

Fast tomographic imaging challenges

Very low signal-to-noise ratio, various errors in projections resulting in inaccurate reconstructions, motion artifacts.

1. Advanced image reconstruction techniques: mathematical methodology, practical challenges
2. Better segmentation methods, object recognition, feature tracking, clustering and labeling
3. Machine learning approaches using data simulated by **TomoPhantom**, application to real data

Fast tomographic imaging challenges

Very low signal-to-noise ratio, various errors in projections resulting in inaccurate reconstructions, motion artifacts.

1. Advanced image reconstruction techniques: mathematical methodology, practical challenges
2. Better segmentation methods, object recognition, feature tracking, clustering and labeling
3. Machine learning approaches using data simulated by **TomoPhantom**, application to real data
4. Development of more advanced physical models to replicate real data errors/artifacts

Example of SLAE for tomography

Let's consider a set of linear equations:

$$\boldsymbol{b} = \mathrm{A}\boldsymbol{x} + \boldsymbol{\delta},$$

where

- $\boldsymbol{b} \in \mathbb{R}^M$ - vectorized sinogram; $M = P\ (2.5\text{k}^2) \times \theta\ (0.9\text{k})$
- $\boldsymbol{x} \in \mathbb{R}^N$ - seeking volume; $N = 2.5\text{k}^3$ voxels
- $\boldsymbol{\delta} \in \mathbb{R}^M$ - random noise
- $\mathrm{A} : \mathbb{R}^N \to \mathbb{R}^M$ - system projection matrix (discrete approximation of the continuous Radon transform for parallel beam geometry)

Example of SLAE for tomography

Let's consider a set of linear equations:

$$\boldsymbol{b} = \mathrm{A}\boldsymbol{x} + \boldsymbol{\delta},$$

where

- $\boldsymbol{b} \in \mathbb{R}^M$ - vectorized sinogram; $M = P\,(2.5\text{k}^2) \times \theta\,(0.9\text{k})$
- $\boldsymbol{x} \in \mathbb{R}^N$ - seeking volume; $N = 2.5\text{k}^3$ voxels
- $\boldsymbol{\delta} \in \mathbb{R}^M$ - random noise
- $\mathrm{A} : \mathbb{R}^N \to \mathbb{R}^M$ - system projection matrix (discrete approximation of the continuous Radon transform for parallel beam geometry)
- For 4D imaging $M(5.6 \times 10^9) << N(1.56 \times 10^{10})$ and A is "fat"

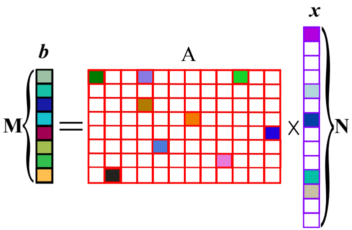

Adding temporal dimension

We have $K > 100$ time frames and for each frame, data $\boldsymbol{b}$ can be regarded as it were obtained from the stationary object.

$$\boldsymbol{B} = \mathbf{A}\boldsymbol{X},$$

where $\boldsymbol{X} := (\boldsymbol{x}_1^\intercal, \ldots, \boldsymbol{x}_K^\intercal)^\intercal$, $\boldsymbol{X} \in \mathbb{R}^{N \times K}$ is a vector containing all $\boldsymbol{x}$ instances of time lapse series and $\boldsymbol{B} := (\boldsymbol{b}_1^\intercal, \ldots, \boldsymbol{b}_K^\intercal)^\intercal$, $\boldsymbol{B} \in \mathbb{R}^{M \times K}$ is a measured projections vector. The block diagonal matrix $\mathbf{A} \in \mathbb{R}^{M \times K \times N \times K}$ is given as:

$$\mathbf{A} = \begin{bmatrix} \mathrm{A}_1 & 0 & \ldots & 0 \\ 0 & \mathrm{A}_2 & & 0 \\ \vdots & & \ddots & \vdots \\ 0 & 0 & \ldots & \mathrm{A}_K \end{bmatrix}$$

We can assume that $\mathbf{A}$ is time-invariant, that is, $\mathrm{A}_1 = \mathrm{A}_2 = \ldots = \mathrm{A}_K$ or $\mathbf{A} = \mathbf{I} \otimes \mathrm{A}_1$, where $\otimes$ is the Kronecker product.

Access to data and software dependencies

Get python scripts, presentations, installation recommendations and related papers from:

https://github.com/dkazanc/ITT_BATH_DLS

- Ice-cream data can be accessed using the script
  ITT_BATH_DLS/DynamicImaging/ICE_CREAM/ITT_IceCreamData.py
- Dendritic data can be accessed using the script
  ITT_BATH_DLS/DynamicImaging/Dendrites/ITT_dendrites.py
- **TomoPhantom** package for data modelling
- **TomoRec** package for image reconstruction

References i

- E. Guo, D. Kazantsev, J. Mo, J. Bent, G. Van Dalen, P. Schuetz, P. Rockett, D. StJohn, and P. D. Lee, *Revealing the microstructural stability of a three-phase soft solid (ice cream) by 4d synchrotron x-ray tomography*, Journal of Food Engineering, (2018).
- E. Guo, A. Phillion, B. Cai, S. Shuai, D. Kazantsev, T. Jing, and P. D. Lee, *Dendritic evolution during coarsening of mg-zn alloys via 4d synchrotron tomography*, Acta Materialia, 123 (2017), pp. 373–382.
- E. Guo, S. Shuai, D. Kazantsev, S. Karagadde, A. Phillion, T. Jing, W. Li, and P. D. Lee, *The influence of nanoparticles on dendritic grain growth in mg alloys*, Acta Materialia, 152 (2018), pp. 127–137.

E. Guo, G. Zeng, D. Kazantsev, P. Rockett, J. Bent, M. Kirkland, G. Van Dalen, D. S. Eastwood, D. StJohn, and P. D. Lee, *Synchrotron x-ray tomographic quantification of microstructural evolution in ice cream–a multi-phase soft solid*, Rsc Advances, 7 (2017), pp. 15561–15573.

D. Kazantsev, E. Guo, A. Phillion, P. J. Withers, and P. D. Lee, *Model-based iterative reconstruction using higher-order regularization of dynamic synchrotron data*, Measurement Science and Technology, 28 (2017), p. 094004.

D. Kazantsev, V. Pickalov, S. Nagella, E. Pasca, and P. J. Withers, *Tomophantom, a software package to generate 2d–4d analytical phantoms for ct image reconstruction algorithm benchmarks*, SoftwareX, 7 (2018), pp. 150–155.